Defect and Diffusion Forum
ISSN: 1662-9507, Vol. 451, pp 147-156
doi:10.4028/p-S43Bos
© 2026 The Author(s). Published by Trans Tech Publications Ltd, Switzerland.
Submitted: 2026-01-19
Accepted: 2026-02-27
Online: 2026-04-17

Determination of Gelation Zone Position in Reactive Thermoplastic Pultrusion by Analysis of Heating Power Consumption

Michael Wilhelm[1,a*], Christoph Schelleis[1,b], Georg Zeeb[1,2,c] and Frank Henning[1,2,d]

[1]Fraunhofer Institute for Chemical Technology (ICT), Joseph-von-Fraunhofer-Str. 7, 76327 Pfinztal, Germany

[2]Karlsruhe Institute of Technology (KIT), Institute of Vehicle Systems Technology (FAST) – Lightweight Engineering, Rintheimer Querallee 2, 76131 Karlsruhe, Germany

[a]michael.wilhelm@ict.fraunhofer.de, [b]christoph.schelleis@ict.fraunhofer.de, [c]georg.zeeb@ict.fraunhofer.de, [d]frank.henning@ict.fraunhofer.de (*corresponding author)

Keywords: pultrusion, reactive thermoplastic, caprolactam, gel zone, power consumption

Abstract. Process speed in pultrusion is significantly influenced by the exothermic reactions of the matrix materials used. The main reaction zone (gel zone) is a key indicator to describe and interpret the reaction behavior in pultrusion. It can be easily observed by elevated temperatures in the die, particularly for highly exothermic thermoset matrices like vinyl ester, epoxy, and polyurethane. However, this effect is not as pronounced in reactive thermoplastics. The exothermic reactions contribute to a reduction in power consumption of the heating plates within the different heating zones, each with its individual temperature. Analyzing the power consumption of the individual heating zones across different process parameter settings allows to determine the position of the gel zone. This information is foundational for pultrusion process optimization, as it allows for more efficient utilization of the die length, ultimately increasing the pull speeds and enabling higher production rates. In this study, a comparative analysis of the power consumption across the heating zones was performed. To validate the findings obtained from the power measurements, thermocouples were drawn through the die at the same process parameters to accurately measure the temperature evolution within the pultruded profile throughout the die length.

Introduction and State of the Art

Motivation. All continuous fiber reinforced plastics (FRPs), typically glass- or carbon-fiber reinforced thermosets, offer several advantages as compared to conventional metallic materials in use due to their superior mechanical performance in combination with a low specific weight in diverse sectors like transportation, consumer goods and others. One method for producing highly filled FRPs is the pultrusion process. The highly filled pultruded profiles with fiber volume content (FVC) up to >70 % can be used in many ways. Cut to the required length, they can already be commissioned as final components (e.g., tent poles) or as local reinforcements in larger structures to specifically improve their mechanical properties.

In the field of matrix systems in pultrusion, unsaturated polyester resins (UP) and vinyl ester resins (VE) make up the largest share with low price and easy processability in open impregnation baths. VE resins are used instead of UP resins when higher mechanical properties and chemical resistance are required. Epoxy resins (EP), primarily EP anhydride resins, have also been used for many decades and offer high mechanical properties due to the strong fiber-matrix interface as well as good chemical and heat resistance. Polyurethanes (PUR) represent the last major matrix group. Featuring a short processing time, they can only be processed with injection chambers and offer particularly good impact strength and mechanical properties [1, 2].

With today's increasing demands on the functionality of materials and components also in subsequent processes, thermoplastics are becoming increasingly important as a matrix material. Also, in high-performance continuously FRPs, due to the possibility of functionalizing them by means of forming, welding or overmolding. Another major advantage is the considerably simpler recycling by

This article is an open access article under the terms and conditions of the Creative Commons Attribution (CC BY) license (https://creativecommons.org/licenses/by/4.0)

chemical or mechanical processes [3]. Although pultrusion with thermoplastic matrices has been the subject of research since the 1980s, pultruded thermoplastic profiles have not been mass-produced as of now [4].

Commonly employed processing routes for thermoplastic profiles can be broadly categorized as non-reactive and reactive processing. In non-reactive processing, already fully polymerized thermoplastics are processed, whereas in reactive processing, polymerization takes place in the pultrusion die, i.e. "in-situ". The reactive processing of the monomer ε-caprolactam which anionically polymerizes to polyamide 6 (aPA6) (so-called "in-situ pultrusion") enables a high fiber content and excellent mechanical properties at competitive raw material costs. Due to the extremely low viscosity of 5 mPa*s to10 mPa*s [5] and the adjustable reactivity by varying activator and catalyst concentrations, efficient impregnation of FVCs of >70 % can be achieved even at pull speeds up to v_{pull} = 3 m/min.

While the in-situ pultrusion process was developed for industrial application within the last few years [6, 7], process optimization is still ongoing to increase productivity and profile quality. During process development, one novel method was found to be promising for optimization of both, productivity and profile quality, at the same time with no direct intervention in the process, which is critical to process stability in pultrusion.

When using reactive matrix systems based on thermosets or thermoplastics, the polymerization takes place while fibers and matrix are being pulled continuously through the die. The state of the matrix as it passes through the die can be divided into three main states: initially liquid, then gel-like and solid after polymerization is complete.

The polymerization of the liquid matrix is initiated by external energy input. Usually, the die is equipped with external heating plates or heating cartridges within the die, separated into several individually adjustable heating zones (HZ). Depending on reaction mechanisms and specific requirements of the matrix system formulation, profile cross section and various other parameters, the temperatures of each individual HZ are set to desired values. After initiation of the polymerization, essentially taking place in the front part of the die, an increase in polymerization rate occurs in the *main polymerization zone*, mostly referred to as *gel zone*. In this gel zone, in addition to the external energy introduced via the heating zones, an often even larger proportion of energy is generated by the exothermic energy released during the polymerization reaction.

Connolly at al. reported for PUR resins in closed injection pultrusion with three HZs that in steady state, zone 2 of 3 is not heated due to the heat generated by the exothermic reaction of the resin curing [2]. Similar, little more pronounced results are reported by Wilhelm [8] who observed an approx. 20 °C higher temperature compared to the set value in the main reaction zone located at HZs 3 and 4 of 6 for an EP anhydride system. With ortophtalic polyester, similar behavior was observed by Tucci et. al, whereby the temperature in zone 3 of 3 in the die was about 8 °C higher due to the exothermic curing of the polyester resin [9]. Same observations were made by Li et al. using VE resin [10] and Cho et al. using ε-caprolactam [11].

The position of the peak exothermy varies over all above-mentioned references mainly between mid and end within the die length. The height of the peak strongly depends on the matrix system used due to different exothermic properties as well as the profile cross sections, FVC and temperature sensor positions. The ideal position of the main polymerization zone depends on the material system and varies slightly between them. Therefore, no standardized optimal position can be defined. However, since all reactive matrices show this significant exothermy, this effect can be used to analyze and optimize the process in terms of productivity and profile quality, using the relative power consumption in form of the *mean control variable* $C_{I,mean}$ of the individual HZs as parameter.

Procedure. In this study, a pultrusion die equipped with six distinct HZs was used. The $C_{I,mean}$ of the power consumption for each HZ was measured to gain insight into the thermal dynamics of the process. Trials were conducted with differing parameter settings to observe their effects on energy consumption. A comparative analysis of the power consumption across the HZs was performed to identify trends and correlations. To validate the findings, thermocouples were drawn through the die

at the same process parameters to accurately measure the temperature evolution within the pultruded profile throughout the entire processing length.

Materials, Processing and Methods

Materials. The study was conducted using StarRov® 2400-886 glass fibers with 2400 tex recommended by Johns Manville for reactive thermoplastic processing. Both reactive components sodium-caprolactamate (Bruggolen C10) as catalyst and hexamethylene-1,6-dicarbamoylcaprolactam (Bruggolen C20P) as activator as well as AP-Nylon caprolactam flakes were from L. Brüggemann GmbH & Co. KG, Heilbronn, Germany.

Processing. A schematic illustration of the pultrusion line used for the investigations is shown in Fig. 1. The glass fibers are pulled through the process line by the caterpillar puller unit of the Nanjing LYT pultrusion line with v_{pull} between v_{pull} = 0.1 m/min - 3.0 m/min. After the fiber rack the fibers are passing through an in-line convection oven of three meters length, equipped with an electrical heater type Leister LHS 61L SYSTEM combined with a medium pressure blower offering an air flow rate of 13.5 m³/min. Upfront of the one meter long, hard chrome plated, state-of-the-art pultrusion die with a 30 x 4 mm² cross section, an injection and impregnation chamber (ii-box) with a tapper angle of 2 x 0.8° was mounted.

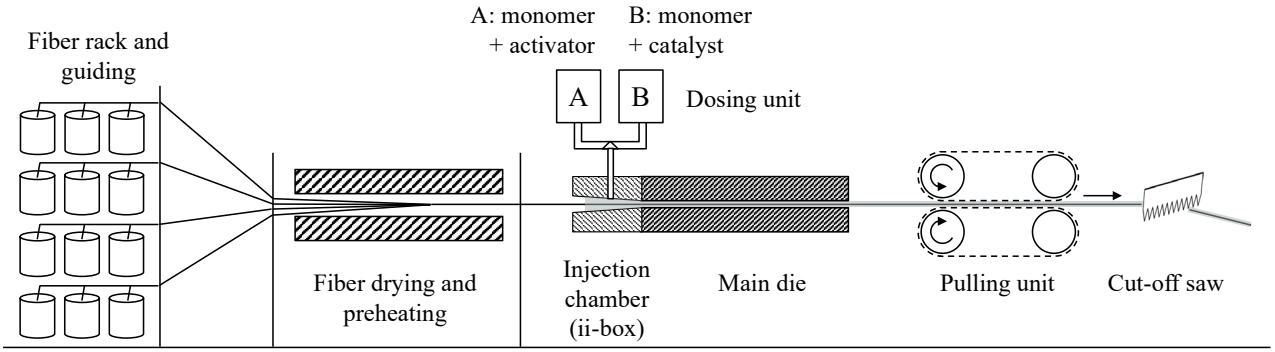

Fig. 1. Schematic drawing of the used pultrusion line setup.

Both on the upper and the lower side of the ii-box and the main die, twelve electric heating plates divided into six HZ were installed as shown in Fig. 2. For temperature control each HZ was equipped with a thermocouple mounted from the side of the die near the cavity. With the precise control of the pultrusion system an accuracy of approx. ± 0.3 °C was achieved. Heating zone 1 is placed on the ii-box, while HZs 2 - 6 heat the main die. Target temperatures for all HZs are summarized in Table 1.

Table 1. Target temperatures for HZ 1 – HZ 6 of the die temperature profile. Heating zone 1 heats the injection chamber, while heating zones 2 - 6 heat the main die.

Die temperature profile	$T_{HZ\,1}$ ii- box	$T_{HZ\,2}$	$T_{HZ\,3}$	$T_{HZ\,4}$	$T_{HZ\,5}$	$T_{HZ\,6}$
	90 °C	100 °C	150 °C	160 °C	170 °C	180 °C

The ii-box is interchangeable. This requires more external mass at the connection point to the main die serving as a potential heat sink. The clamping devices fixing the die on the machine table, also possible heatsinks, influence the heating between HZ 2 and HZ 3 as well as at the die exit at HZ 6.

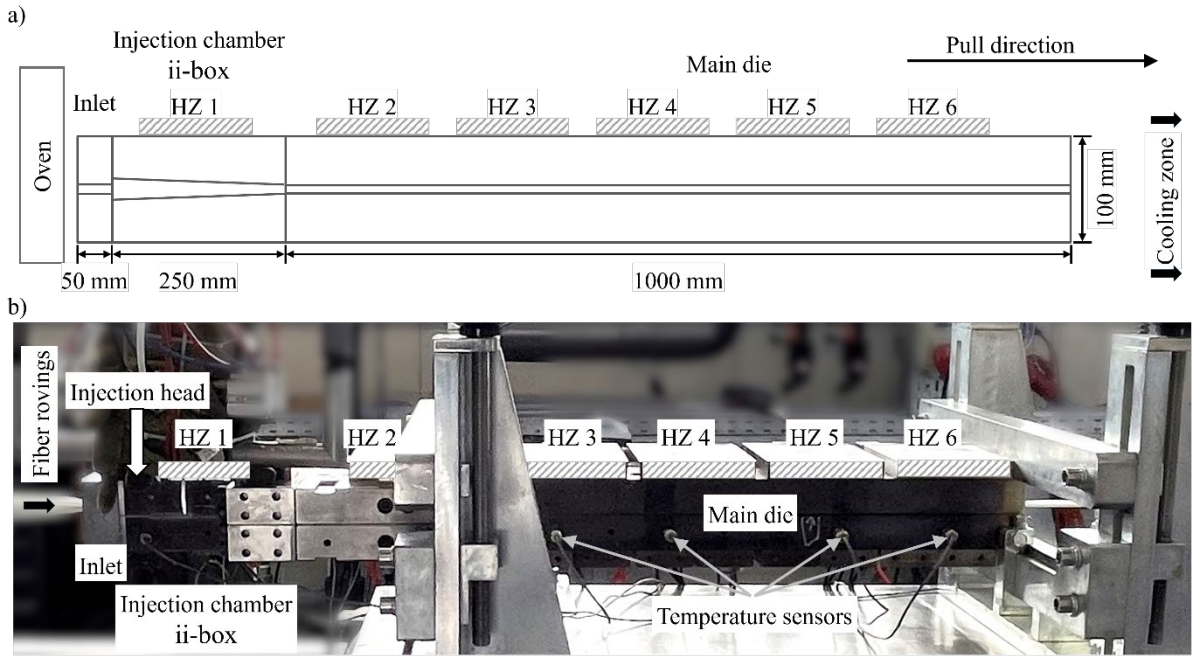

Fig. 2. a) Schematic drawing of the pultrusion die setup with pull direction indicated b) photo of the die on the shop floor.

The parameter settings for this study are based on findings of a comprehensive statistical investigation of Wilhelm [12]. Setting "O1" aims for high profile quality, whereas "O3" focuses on high v_{pull}, see Table 2. The main differences between the two parameter settings are v_{pull} and the concentration of activator (act.) and catalyst. For the simplification only the activator content is given, the catalyst content corresponds to twice the weight of the activator. With the selected process conditions, the concentration of activator and catalyst only has an influence on the reaction rate, but not on the exothermic energy released. This is due to the special nature of the anionic polymerization of ε-caprolactam and has been reported several times [13, 14]. However, the biggest difference between the two parameter settings is v_{pull}, which is nearly five times higher for O3 than for O1.

The pulling speed determines the time available for preheating and drying the fibers as well as their temperature evolution between exiting the oven and entering the injection chamber. Moreover, impregnation and the solidification of the matrix, as well as the available time for polymerization of the matrix within the main die is directly dependent on v_{pull}.

Low v_{pull} reduces economic efficiency. Excessive v_{pull} can lead to an incompletely polymerized matrix, reduced mechanical properties or defects at the surface or in the profile cross-section (pores, cracks) [15, 16]. The settings of O1 and O3 were calculated by the statistical model of [12] aiming for the best profile quality with O1 and giving the highest possible v_{pull} for a quality fulfilling the requirements of DIN EN 13706-2 (E23 profiles) for O3.

Table 2. Processing parameters settings for O1, high profile quality and O3, high v_{pull}.

Trial	T_{dry}	v_{pull}	FVC	Act.	Impregnation pressure	Pull force	rel. dev. Pull force
	in °C	in m/min	in %	in wt.-%	in bar	in kN	in %
O1	202	0.50	69.5	3.00	3.14	2.24	2.80
O3	208	2.59	68.7	3.39	2.52	4.31	2.62

Method and method development. The proposed method aims for the definition of the gel zone position within the pultrusion die or rather the location of peak exothermy by utilizing the power consumption measurement of the HZs.

Reference measurements with dry fibers ("dF") are conducted to achieve a dry steady state with a mass fraction of approx. 0,83 corresponding to the FVC of O1 and O3 without chemical reaction of the matrix for both parameter settings. First, dry fibers are pulled through the setup at nominal speed until a steady state of the temperatures has been reached. With a frequency of 1 Hz, the power consumption data is recorded for 15 min. Based on the data, the *mean control variable* $C_{I,mean}$ of the individual HZs is calculated. The matrix injection is started under constant dry conditions and further data is recorded once a steady state has again been reached. The measurement with injection of reactive matrix ("rM") is carried out for the whole trial duration of 120 min and allows to calculate the difference of $C_{I,mean}$ from dF and rM.

Owing to the mass distribution between the die and the clamping unit (more mass in the connection area of ii-box and main die), the $C_{I,mean}$ of the heating plate control is used for evaluation. In addition, only the relative difference between the reference dF measurement and the rM actual trial is evaluated. The results are validated using the conventional method of pulling through thermocouples that were braided onto fiber rovings in the core of the profile.

In this way, the position of the peak exotherm or rather the position of the gel zone can be determined without invasive sensors. In combination with a correlation of total polymerization conversion and exotherm temperature evolution, this easy-to-implement method could be used to optimize productivity. The relative evaluation also may enable conclusions about batch differences in the matrix or errors in the matrix formulation resulting in an altered reactivity when identical parameters are used.

Results and Discussion

The evaluation of processing parameters in relation to the die heating control variables is discussed first. The course of the measured profile temperature over the entire process length follows.

Fig. 3 shows the average control variables $C_{I,mean}$ of O1 and O3 by HZ 1 to HZ 6. The control variable is a measure of the intensity with which the respective heating zone must be supplied to reach or maintain the defined temperatures, values can be between 0 % and 100 %. Green columns show $C_{I,mean}$ of the two trials over a period of 15 minutes without injection of reactive matrix, i.e., only dry fibers are pulled through the die at the corresponding target speed. The grey columns indicate $C_{I,mean}$ with injection of reactive matrix over the entire remaining trial duration of 120 minutes for both runs.

Running only dF, the influence of the slightly higher drying temperature T_{dry} and the significantly higher v_{pull} of O3 becomes apparent. The pre-heated fibers introduce the entire amount of energy required to reach the set temperature of HZ 1 and HZ 2 resulting in $C_{I,mean}$ = 0 %. For O1 the heating needs to actively input energy to maintain the temperature as the fibers cool down much stronger in the gap between oven and die at 0.5 m/min. This proves that the shorter time in the gap between oven and the die causes less cooling, while significantly more fibers with their associated thermal inertia are pulled through during the same amount of time.

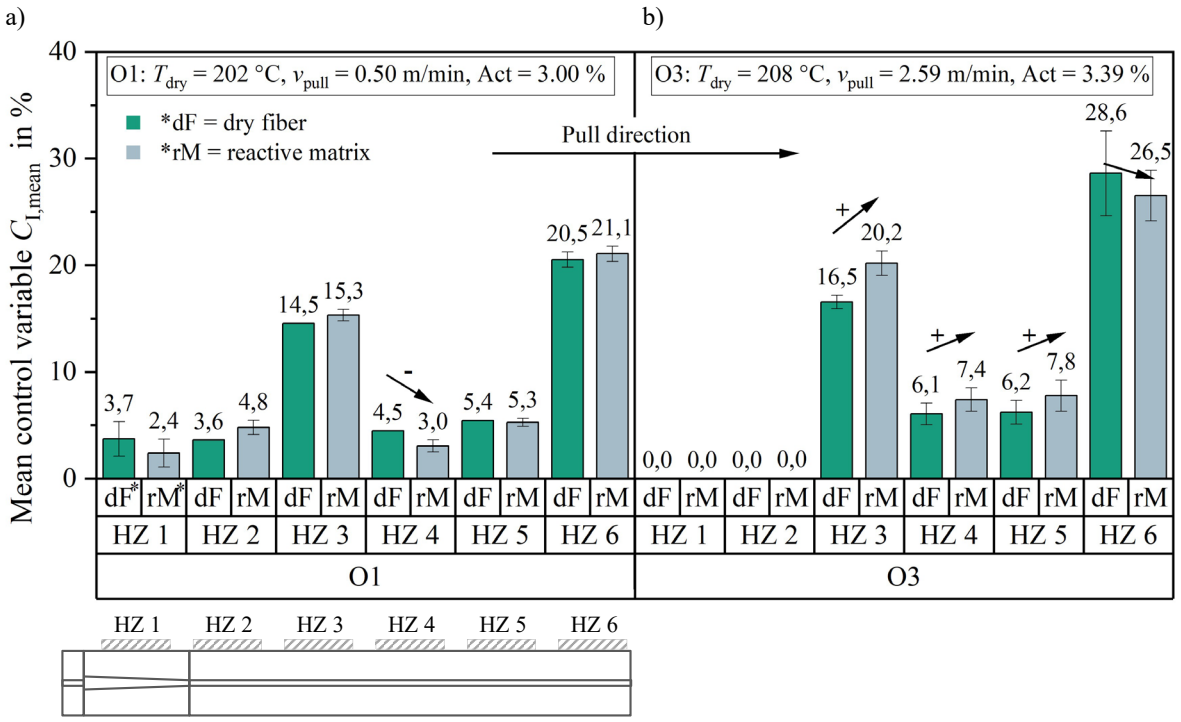

Fig. 3. Comparison of the mean HZ control variables $C_{I,mean}$ in the two runs O1 and O3 with dry fiber and reactive matrix.

The difference in $C_{I,mean}$ is statistically significant (t-test at 0.05 level) for nearly all HZs at both parameter sets, however without clear trend. Averaging across all HZs, $C_{I,mean}$ = 9.7 % for O1 and $C_{I,mean}$ = 9.3 % for O3. This is not statistically significant (t-test at 0.05 level). The dry fibers draw slightly less energy from the die in O3, as they enter the tool hotter due to the higher speed and thereby shorter cooling time after the oven.

In both runs O1 and O3, the matrix is injected into the ii-box at 110 °C in HZ 1 ($T_{HZ\,1}$ = 90 °C). During O1, $C_{I,mean}$ of HZ 3 is only slightly increased by the reactive matrix in contrast to O3, as more mass absorbs more energy and needs to be heated accordingly. For O1 in HZ 4, $C_{I,mean}$ with matrix is 33 % smaller than while processing dry fibers only. This is a clear indication for an exothermic reaction. Heating zones HZ 5 and HZ 6 show almost identical power consumption with and without the matrix. From this result, it can be deduced that the maximum rate of the exothermic polymerization reaction mainly takes place around HZ 4 and subsides in HZ 5 and HZ 6, where it is still slightly supported by external energy input. In the case of O3, significantly more energy is introduced in HZ 3 through HZ 5 running with reactive matrix. Only in HZ 6 the exotherm of the polymerization is visible due to a reduced $C_{I,mean}$. The total heating of the last HZ is significantly stronger during O3 than during O1, although initially no energy input was necessary in the first heating zones. Clearly the mass of matrix that needs to be additionally polymerized predominates.

Fig. 4 shows the measured profile temperature curves $T_{p,m}$ of O1 (green) and O3 (grey) by thermocouples attached to rovings during processing of the reactive matrix relative to their location to the end of the ii-box. Target temperatures, as set, of the die T_{die} (red line) and the drying oven T_{dry} (dashed lines) are shown for both settings O1 and O3. The black, dashed vertical lines in the drying oven visualize fiber guide plates with ceramic eyelets through which the rovings are guided.

Even before entering the drying oven at the position relative to the main tool p_m = -3730 mm, the rovings are heated by the hot air outflow of the oven. In the oven itself, a step-like temperature increase is observed at the fiber guiding plates, as these influence the air flow pattern, which decreases towards the oven entrance. The fibers reach a maximum temperature of 193.4 °C at O1 at the level of the hot air inlet. At O3, a maximum temperature of 186.3 °C is measured slightly offset from the hot air inlet located 700 mm before the oven outlet, i.e., at p_m = -1430 mm. Decreases and increases in temperature before and after the eyelets are particularly noticeable at O1 with low v_{pull}. Between

the outlet of the drying oven and the inlet of the die, the fibers are exposed to the ambient air for a distance of 430 mm resulting in 52 s for O1 and 10 s for O3.

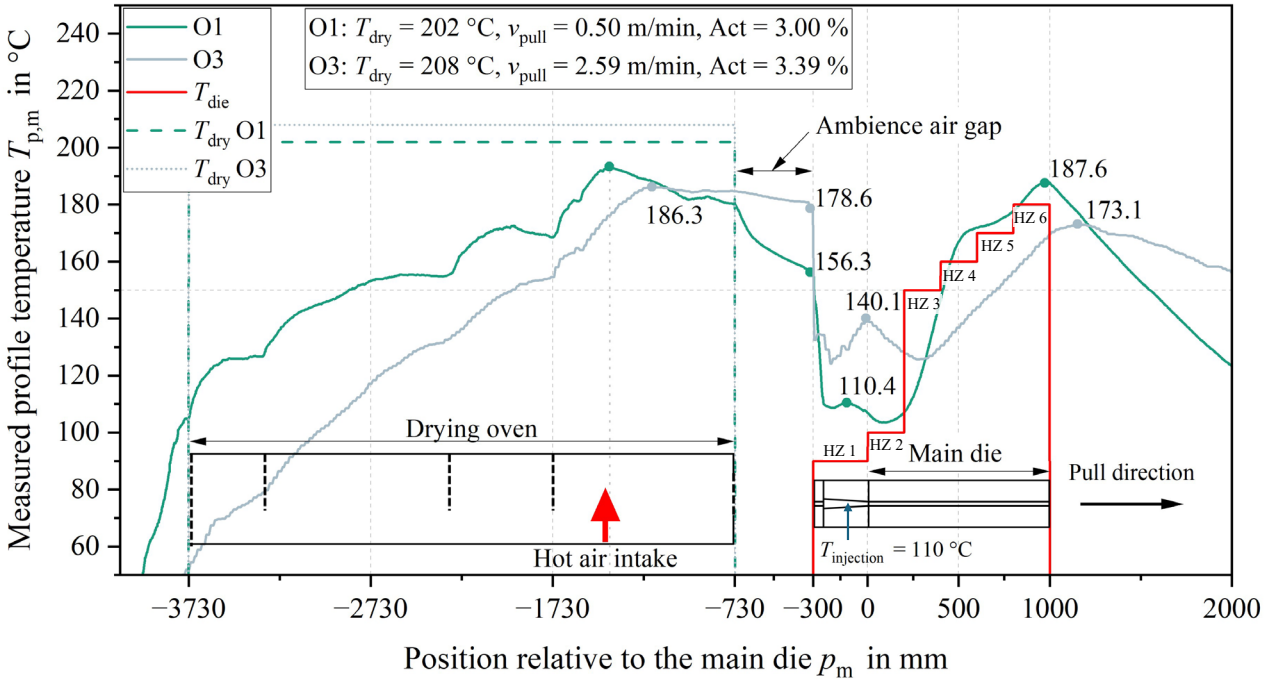

Fig. 4. Temperature $T_{p,m}$ processing reactive matrix for O1 and O3 over relative position p_m.

In this exposed distance, the fibers at O3 maintain a high temperature of 178.6 °C until they enter the die. Due to the five times slower v_{pull}, the fibers from O1 only have a temperature of 156.3 °C when entering the die, which is about 22 °C less compared to O3 and dropping off almost 40 °C from their peak temperature in the oven (193.4 °C).

In both trials, the temperature drops sharply upon entering the mold at p_m = -300 mm. This can be explained by the quasi-static matrix flow front at the ii-box inlet. As the continuous matrix injection is controlled in a manner that the ii-box is always fully filled, the conductive contact of the thermocouple with the 110 °C hot matrix in HZ 1 with $T_{HZ\,1}$ = 90 °C leads to this sharp drop.

After the initial contact in O1, $T_{p,m}$ increases to 110.4 °C in the middle of the ii-box and then drops again. The brief increase is caused by the matrix, which is injected at 110 °C. The drop is due to the mold temperature of HZ 2 at 100 °C (solid red line) which is not compensated by the matrix because of its small amount with just 17 % by mass compared to the fiber mass content of 83 %. T_{die} of HZ 3 is set to the optimum polymerization temperature of approximately 150 °C [17, 18]. Polymerization is initiated and reaches the maximum polymerization rate within a short time, as can be seen from the overshoot of $T_{p,m}$ in HZ 4 at around p_m = 500 mm. The exothermic reaction further heats the profile core, peaking at $T_{p,m}$ = 187.6 °C exiting the mold. The overshoot in HZ 4 correlates with the results of $C_{I,mean}$ in Fig. 3, locating the position of the maximum polymerization rate in HZ 4.

Furthermore, the T_{die} profile appears to be suitable for keeping the polymerization reaction slow initially in HZ 1 and HZ 2 for reliable impregnation and processing, accelerating polymerization significantly from HZ 3 onwards, and continuing to support it until the profile exits the mold.

After entering the tool, O3 generally follows a similar curve to O1, with a temperature rise shortly after entering the ii-box at the injection point to 140.1 °C, followed by a temperature drop to approximately the middle of HZ 3. From HZ 3 to the end of the mold, the temperature curve in the profile lags behind the set temperatures of the mold due to the high v_{pull}. About 140 mm after the mold exit, the maximum profile temperature reached 173.1 °C. In the ii-box, instead of rising to 140.1 °C, a temperature drop to approximately 110 °C (matrix temperature during injection) would be expected for O3. However, it is assumed that this is caused by a deviation in the flow pattern of the matrix in the ii-box due to much higher v_{pull}. The thermocouple is attached to a roving in the center of the saturated fiber package and measures the temperature in the "core" of the profile. This

temperature is higher, because the fibers lost less energy within the ambient air gab due to the higher v_{pull}. This also correlates with the $C_{I,mean} = 0$ of HZ 1 and HZ 2 in O3. The temperature peak after HZ 6 also matches with the results of $C_{I,mean}$ from O3, which show that the exothermic peak only becomes visible from HZ 6 onwards. Since the peak exotherm is behind the tool, it could be assumed that v_{pull} of O3 was selected too high. However, the total conversion is sufficiently high (residual monomer content < 1%), so that the minimum requirements for the profiles are met. The surface quality of the profiles is lower than that of O1, which is not relevant for certain applications. As a result, the parameter setting O3 can also be used to produce industrially viable profiles with significantly higher productivity.

Summary

It was shown that the proposed method by using the relative deviation of the average control variable $C_{I,mean}$ from the heating power consumption, is suitable for determining the position of the main polymerization zone within the die. By pulling through thermocouples connected to rovings to measure the temperature evolution and exotherm heat release, the results were validated successfully. With reference measurements of only dry fibers being processed, heat sinks due to die design or die clamping become negligible.

In O1, polymerization mainly takes place in the middle of the die in the area of HZ 4 and is already very advanced or complete at the end of the die. In O3, polymerization is only completed in the ambient atmosphere after the die, which explains the higher residual monomer content and the observed rougher surface of the manufactured profiles. With both parameter configurations, profiles can be produced in a robust process over the 120 minutes considered. The pulling speed of 0.5 m/min for O1 and 2.59 m/min for O3 represents a wide range in terms of the economic efficiency of the process and roughly indicates the current limits for the process and material parameters considered.

If the exothermic peak is correlated with the degree of conversion of the polymerization reaction for the individual matrix system, this method offers the potential for efficient process optimization in terms of productivity and the use for continuous quality monitoring. For optimization purposes, v_{pull} can be increased for most matrix systems until the exothermic peak is in the range of HZ 5 to HZ 6, in addition to considering several other influencing variables and interactions. This may allow the available die length to be used more efficiently. For quality control, continuous monitoring of the power consumption can be used, for example, to detect differences in the raw material batches or to reveal errors in the matrix formulation if these result in a deviating reactivity.

Key Findings

- The newly proposed method proves to be effective for determining the gel zone in the pultrusion process and can be used for all reactive matrix systems.
- A clear correlation exists between power consumption and the peak exotherm measured by the thermocouples pulled through the die, indicating the reliability of this method.
- This non-invasive and easy-to-implement method offers the potential to be used as process optimization tool as well as for continuous quality control

Acknowledgements

The research documented in this manuscript was funded by the Ministry of Economics, Labor and Tourism Baden-Württemberg (“CaproPULL” Grant No ibwip-BW1_0025). Support from Johns Manville Europe GmbH in the form of trial materials is gratefully acknowledged.

References

[1] S. Strauss *et al.,* "Experimental and Simulative Analysis of the Pressure Development in a Closed Injection Pultrusion Process with Multiple Chamber Geometries," *Polymers*, vol. 15, no. 6, 2023, doi: 10.3390/polym15061544.

[2] M. Connolly, "Pultruding Polyurethane Composite Profiles: Practical Guidelines for Injection Box Design, Component Metering Equipment & Processing," in *Proceedings of COMPOSITES 2005 Convention and Trade Show*, Columbus, Ohio, USA, 2005.

[3] M. Wilhelm, H. Kummert, A. Suratkar, P. Rosenberg, and F. Henning, "A study on the mechanical recycling of continuous glass fibre reinforced nylon 6 profiles produced by in-situ pultrusion," in *Proceedings of SAMPE Europe*, Madrid, Spain, 2023. [Online]. Available: doi:// 10.24406/publica-2006

[4] K. Minchenkov, A. Vedernikov, A. Safonov, and I. Akhatov, "Thermoplastic Pultrusion: A Review," *Polymers*, vol. 13, no. 2, 2021, doi: 10.3390/polym13020180.

[5] S. Russo and E. Casazza, "Ring-Opening Polymerization of Cyclic Amides (Lactams)," in *Polymer Science: A Comprehensive Reference*, M. Moeller and K. Matyjaszewski, Eds., Amsterdam, Niederlande: Elsevier, 2012, pp. 331–396. [Online]. Available: doi://10.1016/ B978-0-444-53349-4.00109-6

[6] M. Wilhelm, G. Zeeb, P. Rosenberg, and F. Henning, "In-situ Pultrusion of Nylon 6 Based Profiles - Key Parameters of the Process," in *Proceedings of 9th annual CAMX – The Composites and Advanced Materials Expo*, Atlanta, USA, 2023. [Online]. Available: doi.org/10.33599/nasampe/c.23.0095

[7] F. Behnisch, M. Wilhelm, and M. Janssen, "Cost-effective and recyclable: functionalized aPA6 profiles in injection molding," Mannheim, Jun. 20 2024.

[8] F. Wilhelm, "Einsatz von Leistungsultraschall in der geschlossenen Injektions-Pultrusion," Dissertation, Technische Universität München, 2021.

[9] F. Tucci, V. Esperto, F. Rubino, and P. Carlone, "Experimental Measurement of the Resistant Load in Injection Pultrusion Processes," *Procedia Manufacturing*, vol. 47, pp. 148–153, 2020, doi: 10.1016/j.promfg.2020.04.157.

[10] S. Li, L. Xu, Z. Ding, L. J. Lee, and H. Engelen, "Experimental and Theoretical Analysis of Pulling Force in Pultrusion and Resin Injection Pultrusion (RIP)–Part I: Experimental," *Journal of Composite Materials*, vol. 37, no. 2, pp. 163–189, 2003, doi: 10.1106/002199803028676.

[11] B.-G. Cho, S. P. McCarthy, J. P. Fanucci, and S. C. Nolet, "Fiber reinforced nylon-6 composites produced by the reaction injection pultrusion process," *Polym Compos*, vol. 17, no. 5, pp. 673–681, 1996, doi: 10.1002/pc.10659.

[12] M. Wilhelm, "Verfahrensentwicklung für die Herstellung kontinuierlich faserverstärkter, thermoplastischer Profile im Pultrusionsverfahren mittels in-situ Polymerisation von ε Caprolactam," Dissertation, Karlsruher Institut für Technologie (KIT), 2025.

[13] M. Wilhelm, R. Wendel, M. Aust, P. Rosenberg, and F. Henning, "Compensation of Water Influence on Anionic Polymerization of ε-Caprolactam: 1. Chemistry and Experiments," *J. Compos. Sci.*, vol. 4, no. 1, pp. 7–26, 2020, doi: 10.3390/jcs4010007.

[14] K. Chen, M. Jia, S. Hua, and P. Xue, "Optimization of initiator and activator for reactive thermoplastic pultrusion," *J Polym Res*, vol. 26, no. 2, p. 40, 2019, doi: 10.1007/s10965-019-1708-6.

[15] A. Vedernikov *et al.,* "Effects of high pulling speeds on mechanical properties and morphology of pultruded GFRP composite flat laminates," *Composite Structures*, vol. 301, 2022, doi: 10.1016/j.compstruct.2022.116216.

[16] M. Volk, J. Wong, S. Arreguin, and P. Ermanni, "Pultrusion of large thermoplastic composite profiles up to Ø 40 mm from glass-fibre/PET commingled yarns," *Composites Part B: Engineering*, vol. 227, 2021, doi: 10.1016/j.compositesb.2021.109339.

[17] M. Narita, H. Yoneyama, T. Matsunaga, and M. Harada, "Simultaneous study of anionic polymerization of ε-caprolactam and crystallization of polyamide 6 in an isothermal process by in situ WAXS," *Polym J*, vol. 52, no. 2, pp. 199–206, 2020, doi: 10.1038/s41428-019-0262-8.

[18] K. van Rijswijk, H. E. N. Bersee, A. Beukers, S. J. Picken, and A. A. van Geenen, "Optimisation of anionic polyamide-6 for vacuum infusion of thermoplastic composites: Influence of polymerisation temperature on matrix properties," *Polymer Testing*, vol. 25, no. 3, pp. 392–404, 2006, doi: 10.1016/j.polymertesting.2005.11.008.